Mechanism for the Direct Oxidation of Benzene to Phenol by FeO^+

Yoshihito Shiota, Kunihiko Suzuki, and Kazunari Yoshizawa*

Institute for Materials Chemistry and Engineering, Kyushu University, Fukuoka 812-8581, Japan

Received February 23, 2005

Reaction pathways and energetics for the conversion of benzene to phenol by FeO^+ in the gas phase are discussed using density functional theory calculations at the B3LYP/6-311+G** level of theory. Three reaction pathways are available for this reaction. The first one is a nonradical mechanism to form a hydroxo intermediate, $HO-Fe^+-C_6H_5$, via H atom abstraction with a four-centered transition state, which occurs at a coordinatively unsaturated metal center. The second one is a radical mechanism to form a phenyl radical and an FeOH fragment as an intermediate via H-atom abstraction with a linear C−H−O transition state. The third one is an oxygen-insertion mechanism to form an arenium intermediate via electrophilic aromatic addition. The energies of the transition states with respect to H-atom abstraction (relative to the dissociation limit) increase in the order of the first, third, and second mechanisms. A detailed analysis of the potential energy surfaces shows that the first mechanism is most likely to occur when the metal active site is coordinatively unsaturated. The second mechanism is energetically unlikely. The third pathway is branched into cyclohexadienone and benzene oxide, which are formed by a 1,2-hydrogen migration and a ring closure in the arenium intermediate, respectively. Cyclohexadienone can play a role as an intermediate when the metal active site is coordinatively saturated, whereas the formation of benzene oxide is unlikely to occur under ambient conditions because of its extremely high energy.

Introduction

Selective oxidation of hydrocarbons is one of the most important subjects in modern chemistry.[1−5] Phenol is now manufactured from benzene using the cumene hydroperoxide process developed in the early 1950s.[6] Although it represented a completely new approach to phenol manufacture, the success of this method is dependent on the byproduct acetone in this process. For this reason, the direct oxidation of benzene is attractive in the production of phenol without byproducts. Aromatic hydrocarbons are enzymatically converted into corresponding phenols by cytochrome P450[7] and by phenylalanine hydroxylase.[8] Thus, both heme and nonheme iron active centers play an important role in the catalytic oxidation of aromatic hydrocarbons. Schwarz and co-workers[9] demonstrated from a mass spectroscopic analysis that the reaction between the bare FeO^+ complex and benzene leads to phenol in the gas phase under ion cyclotron resonance conditions. The FeO^+ complex is of great interest for mechanistic study because it is the simplest model among many oxidation catalysts. Panov and co-workers[10] showed that the iron-containing zeolite Fe−ZSM-5 has great activity as a catalyst for the conversion of benzene to phenol. The active species called α-oxygen is a key in the selective oxidation mediated by Fe−ZSM-5 zeolite. It is reasonable to view the α-oxygen species as an iron-oxo species because this species is produced from the decomposition of N_2O over Fe−ZSM-5 zeolite as in the gas-phase reaction between Fe^+ and N_2O.

Despite an accumulation of many experimental facts, our knowledge on the mechanism of the direct oxidation of benzene to phenol is rather limited. As indicated in Scheme 1, mechanistic proposals for the hydroxylation by metal oxides involve a radical pathway via H-atom abstraction[11] and an oxygen-insertion pathway that

* To whom correspondence should be addressed. E-mail: kazunari@ms.ifoc.kyushu-u.ac.jp.

(1) (a) Shilov, A. E. *The Activation of Saturated Hydrocarbons by Transitions Metal Complexes*; Reidel Publishing: Dordrecht, The Netherlands, 1984. (b) Shilov, A. E.; Shul'pin, G. B. *Chem. Rev.* **1997**, *97*, 2879.

(2) (a) Crabtree, R. H. *The Organometallic Chemistry of the Transition Metals*; Wiley: New York, 1990. (b) Crabtree, R. H. *Chem. Rev.* **1985**, *85*, 245. (c) Crabtree, R. H. *Chem. Rev.* **1995**, *95*, 987.

(3) (a) Eller, K.; Schwarz, H. *Chem. Rev.* **1991**, *91*, 1121. (b) Schröder, D.; Schwarz, H. *Angew. Chem., Int. Ed. Engl.* **1995**, *34*, 1973.

(4) Hill, C. L., Ed. *Activation and Functionalization of Alkanes*; Wiley: New York, 1989.

(5) Davies, J. A.; Watson, P. L.; Liebman, J. F.; Greenberg, A. *Selective Hydrocarbon Activation*; VCH: New York, 1990.

(6) Tyman, J. P. H. *Synthetic and Natural Phenols*; Elsevier: Amsterdam, 1996.

(7) (a) Bush, E. D.; Trager, W. F. *J. Med. Chem.* **1985**, *28*, 992. (b) Korzekwa, K. R.; Swinney, D. C.; Trager, W. F. *Biochemistry* **1989**, *28*, 9019.

(8) (a) Kaufman, S. *Methods Enzymol.* **1970**, *17A*, 603. (b) Kaufman, S. *Metabolism of Aromatic Amino Acids and Amines*; Academic Press: New York, 1987.

(9) (a) Schröder, D.; Schwarz, H. *Helv. Chim. Acta* **1992**, *75*, 1281. (b) Becker, H.; Schröder, D.; Zummack, W.; Schwarz, H. *J. Am. Chem. Soc.* **1994**, *116*, 1096. (c) Ryan, M. F.; Stöckigt, D.; Schwarz, H. *J. Am. Chem. Soc.* **1994**, *116*, 9565.

(10) (a) Panov, G. I.; Sobolev, V. I.; Kharitonov, A. S. *J. Mol. Catal.* **1990**, *61*, 85. (b) Sobolev, V. I.; Panov, G. I.; Kharitonov, A. S.; Romannikov, V. N.; Volodin, A. M.; Ione, K. G. *J. Catal.* **1993**, *139*, 435. (c) Volodin, A. M.; Bolshov, V. A.; Panov, G. I. *J. Phys. Chem.* **1994**, *98*, 7548.

10.1021/om050136b CCC: $30.25
Publication on Web 06/08/2005

Scheme 1

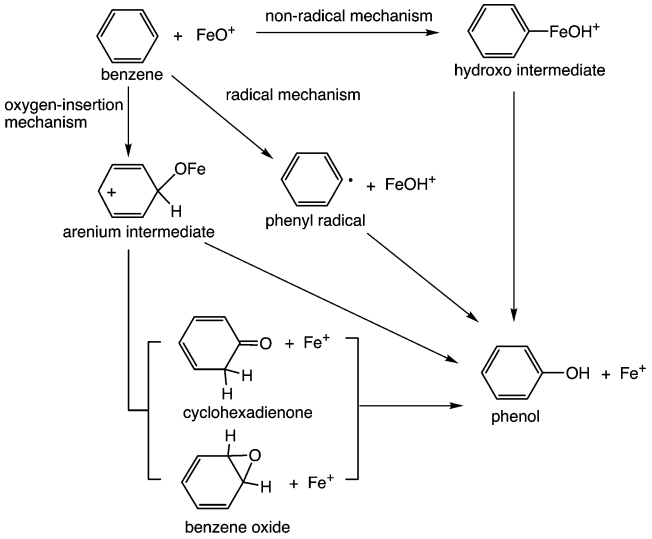

leads to arene oxide as an intermediate.[12] No kinetic isotope effects (KIE) were reported for the oxidation of the benzene ring by FeO^+,[9] aromatic amino acid hydroxylases,[13] and Fe−ZSM-5 zeolite,[14] whereas large KIE values were observed for the hydroxylation of the benzylic C−H bond.[15,16] These results may suggest that the C−H bond dissociation is not the rate-determining step in the course of benzene hydroxylation, while it is rate determining in the hydroxylation at the benzylic position.

We previously proposed a nonradical mechanism for benzene hydroxylation by the bare FeO^+ species with density functional theory (DFT) calculations.[17] In the first half of the proposal H-atom abstraction occurs with a four-centered transition state to form a nonradical intermediate, $C_6H_5-Fe^+-OH$, as shown in Scheme 1. The second half is the recombination of the C_6H_5 and OH ligands with a three-centered transition state at the metal center to form the phenol complex $Fe^+(C_6H_5OH)$. Of course, this mechanism is applicable when the metal active center is coordinatively unsaturated. Although theoretical calculations concerning benzene hydroxylation by various iron-oxo species were recently carried out,[18−20] our knowledge on the activation of the benzene C−H bond is still lacking for the mechanism. The purpose of this study is to study the three possible mechanisms for the benzene-to-phenol conversion in Scheme 1 from the energetic point of view using DFT calculations on $FeO^+ + C_6H_6$.

Method of Calculation

We optimized local minima and saddle points on the potential energy surfaces in the sextet and quartet spin states using the B3LYP method.[21,22] We used the (16s10p6d) primitive set of Wachters−Hay[23,24] supplemented with one polarization f-function ($\alpha = 1.05$ for Fe)[25] for the Fe atom and the 6-311+G** basis set[26] for the H, C, and O atoms. The program we used is Gaussian 03 (Rev. B.03).[27] After geometry optimizations, we performed vibrational analyses to confirm that an optimized geometry corresponds to a local minimum that has no imaginary frequency or a transition state that has only one imaginary frequency.

Results and Discussion

The reaction of benzene with FeO^+ is initiated by H-atom abstraction or oxygen insertion, which can start from the formation of benzene complex $OFe^+(C_6H_6)$ with various structures. In this section we consider the three reaction pathways indicated in Scheme 1: a nonradical mechanism, a radical mechanism, and an oxygen-insertion mechanism. We compare the energetics of these mechanisms in particular with respect to the activation of the strong C−H bond of benzene.

Nonradical Mechanism. Let us first look at a nonradical mechanism via the formation of a hydroxo intermediate, $HO-Fe^+-C_6H_5$. In the initial stages of the reaction the FeO^+ complex approaches the benzene ring to form a benzene complex (B1), which is a kind of π complex. A subsequent H-atom abstraction from the benzene molecule via a four-centered transition state (TS1) results in the formation of a hydroxo intermediate (H). This intermediate is transformed into a phenol complex (P), $Fe^+(C_6H_5OH)$, via a three-centered transition state (TS2), followed by dissociation into phenol and Fe^+. These elementary processes involve neither radical nor ionic species.

Figure 1 shows energies of the intermediates and transition states relative to the dissociation limit along the reaction pathway in the high-spin sextet and low-spin quartet states. General profiles of the high-spin and

(11) Iwamoto, M.; Hirata, J.; Matsukami, K.; Kagawa, S. *J. Phys. Chem.* **1983**, *87*, 903.
(12) (a) Guroff, G.; Daly, J. W.; Jerina, D. M.; Renson, J.; Witkop, B.; Udenfriend, S. *Science* **1967**, *157*, 1524. (b) Jerina, D. M.; Daly, J. W. *Science* **1974**, *185*, 573.
(13) (a) Guroff, G.; Levitt, M.; Daly, J.; Udenfriend, S. *Biochem. Biophys. Res. Commun.* **1966**, *25*, 253. (b) Renson, J.; Daly, J.; Weissbach, H.; Witkop, B.; Udenfriend, S. *Biochem. Biophys. Res. Commun*. **1966**, *25*, 504.
(14) Dubkov, K. A.; Sobolev, V. I.; Talsi, E. P.; Rodkin, M. A.; Watkins, N. H.; Shteinman, A. A.; Panov, G. I. *J. Mol. Catal. A* **1997**, *123*, 155.
(15) Schröder, D.; Florencio, H.; Zummack, W.; Schwarz, H. *Helv. Chim. Acta* **1992**, *75*, 1792.
(16) Hanzlik R. P.; Ling, K.-H. J. *J. Org. Chem.* **1990**, *55*, 3992.
(17) Yoshizawa, K.; Shiota, Y.; Yamabe, T. *J. Am. Chem. Soc.* **1999**, *121*, 147.
(18) de Visser, S. P.; Shaik, S. *J. Am. Chem. Soc.* **2003**, *125*, 7413.
(19) (a) Bathelt, C. M.; Ridder, L.; Mulholland, A. J.; Harvey, J. N. *J. Am. Chem. Soc.* **2003**, *125*, 15004. (b) Bathelt, C. M.; Ridder, L.; Mulholland, A. J.; Harvey, J. N. *Org. Biomol. Chem.* **2004**, *2*, 2998.
(20) Kachurovskaya, N. A.; Zhidomirov, G. M.; van Santen, R. A. *J. Phys. Chem. B* **2004**, *108*, 5944.
(21) (a) Becke, A. D. *Phys. Rev. A* **1988**, *38*, 3098. (b) Becke, A. D. *J. Chem. Phys.* **1993**, *98*, 5648.
(22) Lee, C.; Yang, W.; Parr, R. G. *Phys. Rev. B* **1988**, *37*, 785.
(23) Wachters, A. J. H. *J. Chem. Phys.* **1970**, *52*, 1033.
(24) Hay, P. J. *J. Chem. Phys.* **1977**, *66*, 4377.
(25) Raghavachari, K.; Trucks, G. W. *J. Chem. Phys.* **1989**, *91*, 1062.
(26) Krishnan, R.; Binkley, J. S.; Seeger, R.; Pople, J. A. *J. Chem. Phys.* **1980**, *72,* 650.
(27) Frisch, M. J.; Trucks, G. W.; Schlegel, H. B.; Scuseria, G. E.; Robb, M. A.; Cheeseman, J. R.; Montgomery, J. A., Jr.; Vreven, T.; Kudin, K. N.; Burant, J. C.; Millam, J. M.; Iyengar, S. S.; Tomasi, J.; Barone, V.; Mennucci, B.; Cossi, M.; Scalmani, G.; Rega, N.; Petersson, G. A.; Nakatsuji, H.; Hada, M.; Ehara, M.; Toyota, K.; Fukuda, R.; Hasegawa, J.; Ishida, M.; Nakajima, T.; Honda, Y.; Kitao, O.; Nakai, H.; Klene, M.; Li, X.; Knox, J. E.; Hratchian, H. P.; Cross, J. B.; Bakken, V.; Adamo, C.; Jaramillo, J.; Gomperts, R.; Stratmann, R. E.; Yazyev, O.; Austin, A. J.; Cammi, R.; Pomelli, C.; Ochterski, J. W.; Ayala, P. Y.; Morokuma, K.; Voth, G. A.; Salvador, P.; Dannenberg, J. J.; Zakrzewski, V. G.; Dapprich, S.; Daniels, A. D.; Strain, M. C.; Farkas, O.; Malick, D. K.; Rabuck, A. D.; Raghavachari, K.; Foresman, J. B.; Ortiz, J. V.; Cui, Q.; Baboul, A. G.; Clifford, S.; Cioslowski, J.; Stefanov, B. B.; Liu, G.; Liashenko, A.; Piskorz, P.; Komaromi, I.; Martin, R. L.; Fox, D. J.; Keith, T.; Al-Laham, M. A.; Peng, C. Y.; Nanayakkara, A.; Challacombe, M.; Gill, P. M. W.; Johnson, B.; Chen, W.; Wong, M. W.; Gonzalez, C.; Pople, J. A. *Gaussian 03*, revision B.03; Gaussian, Inc.: Wallingford, CT, 2004.

Table 1. Calculated Mulliken Atomic Charges for the Reaction Species in the Nonradical and Radical Mechanisms (values in parentheses are atomic spin densities)

entry	B1	TS1	H	TS2	P	B2	TS3	R	TS4
sextet									
Fe	0.60	0.71	0.33	0.63	0.64	0.63	0.68	0.90	0.80
	(3.80)	(3.61)	(4.18)	(4.21)	(4.94)	(3.76)	(3.72)	(3.75)	(4.13)
O	−0.22	0.03	−0.16	−0.05	0.02	−0.22	0.09	−0.05	−0.01
	(1.08)	(0.82)	(0.36)	(0.24)	(−0.01)	(0.62)	(0.43)	(0.37)	(0.13)
substrate	0.62	0.27	0.83	0.43	0.34	0.59	0.23	0.15	0.21
	(0.12)	(0.57)	(0.46)	(0.55)	(0.07)	(0.62)	(0.85)	(0.88)	(0.74)
quartet									
Fe	0.52	0.71	0.55	0.73	0.78	0.59	0.86	0.97	0.89
	(3.39)	(3.10)	(3.63)	(3.22)	(2.99)	(3.61)	(3.57)	(3.57)	(3.49)
O	−0.22	0.14	−0.21	−0.04	−0.10	−0.28	−0.02	−0.06	−0.09
	(−0.49)	(0.07)	(0.23)	(−0.04)	(0.00)	(0.11)	(0.23)	(0.29)	(0.24)
substrate	0.71	0.15	0.66	0.31	0.32	0.68	0.16	0.09	0.20
	(0.10)	(−0.17)	(−0.86)	(−0.18)	(0.01)	(−0.72)	(−0.80)	(−0.86)	(−0.74)

low-spin surfaces can be explained by two-state reactivity.[28] Although the ground sextet state of FeO^+ lies 9.7 kcal/mol below the quartet state, the sextet potential energy surface lies well above the quartet one in the vicinity of TS1 and TS2. Therefore the quartet potential energy surface should play an essential role in this reaction as in methane hydroxylation by FeO^+ if spin inversion between the two states takes place.[29] The benzene molecule in the initially formed complex is slightly distorted by the significant interaction with the FeO^+ complex. Table 1, which summarizes computed atomic charges and spin densities based on the Mulliken population analysis, suggests that a significant electron transfer occurs from the benzene molecule to the FeO^+ complex.

The first transition state TS1 is related to the important electronic process responsible for the C−H bond dissociation of benzene. It connects the benzene complex and the hydroxo intermediate and has an imaginary frequency mode of 1791i (1596i) cm^{-1} in the sextet (quartet) spin state. This high frequency is a direct consequence of a C−H bond cleavage as well as an O−H bond formation, as the vibrational mode suggests. The four-centered structure involves a C−H bond of 1.330 (1.360) Å and an O−H bond of 1.226 (1.327) Å in the sextet (quartet) state. These bond distances are reasonable for a transition-state structure responsible for the cleavage of a C−H bond and the formation of an O−H bond. Computed activation energies of TS1 in the sextet and quartet states are 48.4 and 37.5 kcal/mol relative to the initial benzene complex, respectively. However, since the energies of ^{6}TS1 and ^{4}TS1 are −9.2 and −19.0 kcal/mol, respectively, relative to the dissociation limit of FeO^+ ($^6\Sigma^+$) + C_6H_6, this H-atom abstraction should take place in the gas phase substantially with no barrier. The resultant hydroxo intermediate involves an Fe−C bond of 1.931 Å in the sextet state and 2.014 Å in the quartet state. The potential energy diagrams suggest that the surface crossing can occur in the vicinity of TS1.

The second half of the reaction is responsible for the formation of the phenol complex via TS2, which is a transition state for the dissociation of an Fe−C bond and the formation of a C−O bond. The imaginary frequencies of 415i cm^{-1} in the sextet spin state and of 390i cm^{-1} in the quartet spin state tell us that this three-centered transition state correctly connects the hydroxo intermediate and the phenol complex. Computed activation energies of TS2 are 32.0 and 20.1 kcal/mol in the sextet and quartet states, respectively, relative to the hydroxo intermediate. However, TS2 lies well below the dissociation limit, and therefore the reacting system is able to pass over this transition state. Taking the spin inversion into account, a computed overall energy for the formation of the phenol complex is 65.4 kcal/mol exothermic. Thus, these results lead us to conclude that the direct oxidation of benzene to phenol can occur in a nonradical manner if the iron active center of catalysts is coordinatively unsaturated.[17,30]

Radical Mechanism. Usual radical mechanisms involve an H-atom abstraction step with a transition state of a linear C−H−O array in the initial stages of the reaction. First this mechanism requires a direct attack of an H atom of the benzene ring to form a phenyl radical and an FeOH fragment as an intermediate, as indicated in Scheme 1. Second, the recombination of these species results in the formation of alcohol. This mechanism is well known as a radical rebound mechanism, which was initially proposed to explain the catalytic mechanism of alkane hydroxylation by cytochrome P450.[31] Figure 2 shows computed energy diagrams for this reaction mechanism in the sextet and quartet states. Another initial benzene complex (B2) that corresponds to a local minimum on the potential energy surface is the starting point in the radical mechanism. This complex has relative energies of −18.1 and −19.2 kcal/mol in the sextet and quartet spin states, respectively. The radical intermediate (R) is formed via TS3, which has a nearly linear C−H−O array, as expected from a conventional radical mechanism. Computed C−H bond distances in the sextet and quartet states are 1.322 and 1.332 Å, respectively; O−H bond distances in the sextet and quartet states are 1.222 and 1.195 Å, respectively. These bond distances are similar to those of TS1 in the nonradical mechanism and are also reasonable for the cleavage of a C−H bond and the formation of an O−H bond. The direct interaction

(28) (a) Shaik, S.; Danovich, D.; Fiedler, A.; Schröder, D.; Schwarz, H. *Helv. Chim. Acta* **1995**, *78*, 1393. (b) Schröder, D.; Shaik, S.; Schwarz, H. *Acc. Chem. Res*. **2000**, *33*, 139.

(29) Shiota, Y.; Yoshizawa, K. *J. Chem. Phys.* **2003**, *118*, 5872.

(30) (a) Yoshizawa, K.; Yumura, T.; Shiota, Y.; Yamabe, T. *Bull. Chem. Soc. Jpn.* **2000**, *73*, 29. (b) Yoshizawa, K.; Shiota, Y.; Yumura, T.; Yamabe, T. *J. Phys. Chem. B* **2000**, *104*, 734. (c) Yoshizawa, K.; Shiota, Y.; Kamachi, T. *J. Phys. Chem. B* **2003**, *107*, 11404.

(31) (a) Groves, J. T.; Haushalter, R. C.; Nakamura, M.; Nemo, T. E.; Evans, B. J. *J. Am. Chem. Soc.* **1981**, *103*, 2884. (b) Groves, J. T. *J. Chem. Educ.* **1985**, *62*, 928.

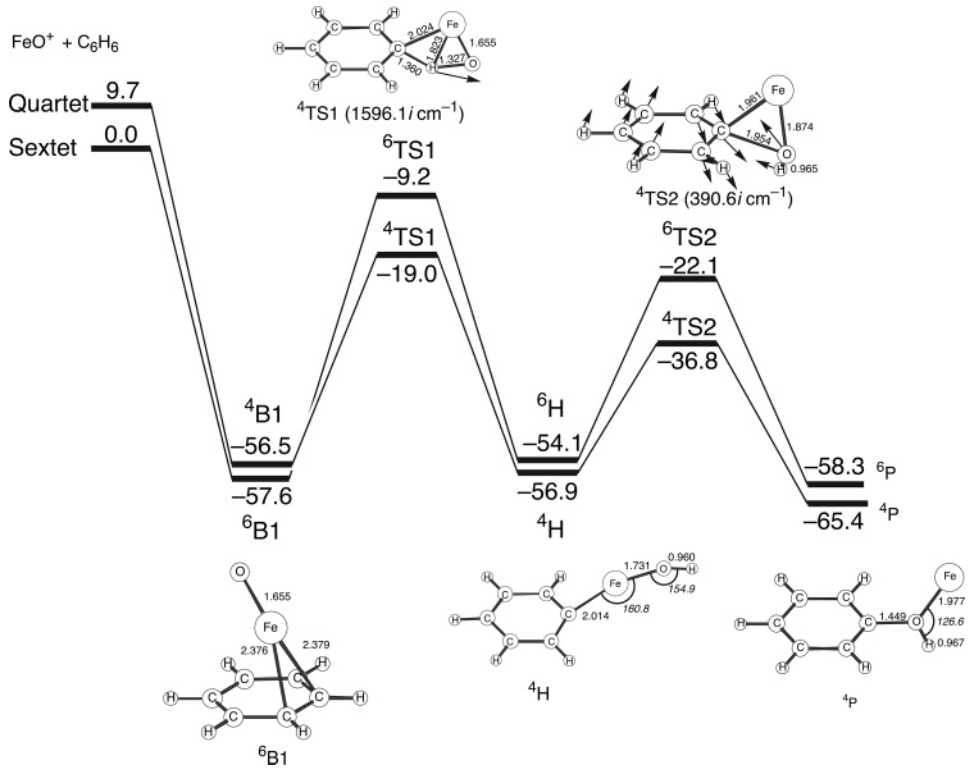

Figure 1. Energy diagrams for benzene hydroxylation along the nonradical mechanism at the B3LYP level of theory. Units are in kcal/mol.

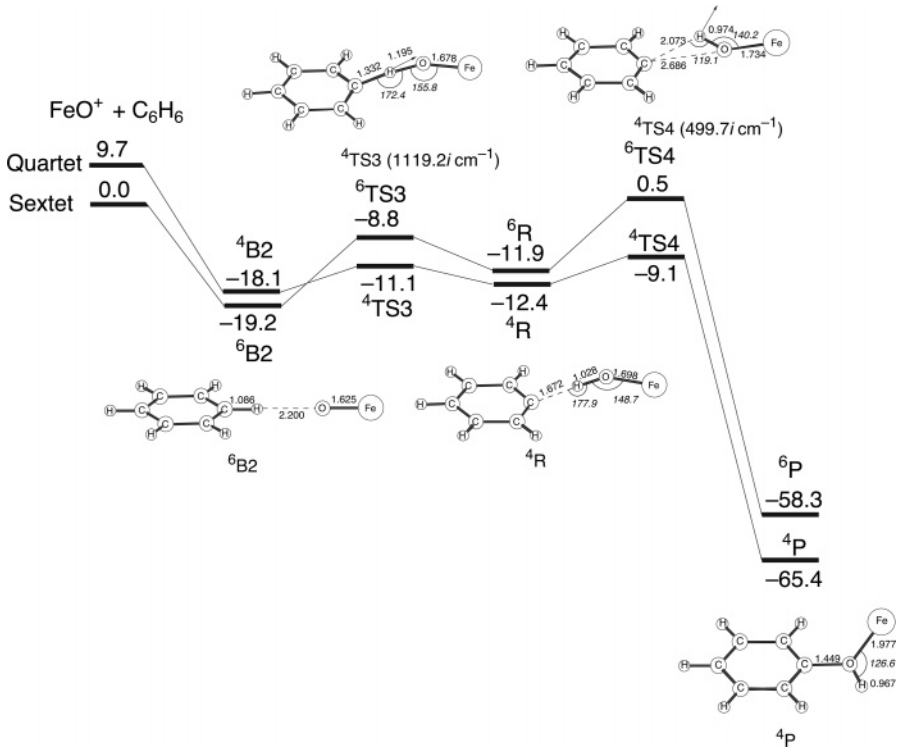

Figure 2. Energy diagrams for benzene hydroxylation along the radical mechanism at the B3LYP level of theory. Units are in kcal/mol.

between the Fe atom and the benzene ring is a key to understanding the H-atom abstraction in the nonradical pathway and the radical pathway. As listed in Table 1, the resultant radical intermediate in the sextet and quartet states has large spin densities of +0.88 and −0.86 on the phenyl radical moiety, respectively, which is weakly bonded to the hydrogen atom of the FeOH moiety. The radical intermediate R is transformed into the phenol complex via a transition state (TS4) for the formation of a C−O bond.

We see in Figure 2 that crossing of the two potential energy surfaces can occur between B2 and TS3. The activation energy for the H-atom abstraction is 10.4 kcal/mol on the sextet potential energy surface, while it is decreased to 8.1 kcal/mol if we take the spin inversion into account. Therefore the spin inversion can

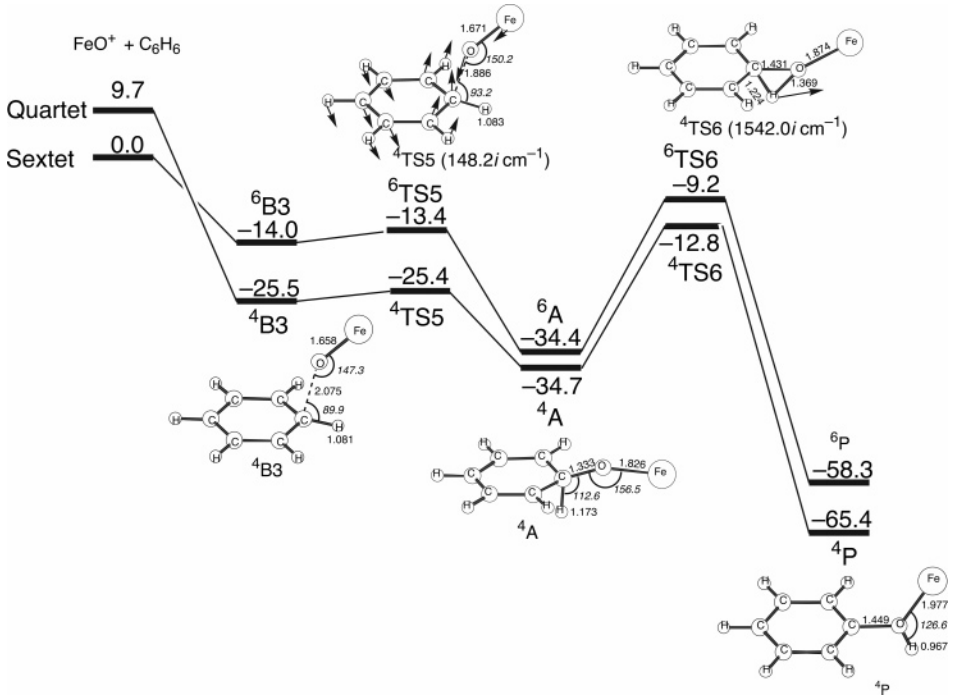

Figure 3. Energy diagrams for benzene hydroxylation along the oxygen-insertion mechanism at the B3LYP level of theory. Units are in kcal/mol.

play an important role in the C−H bond cleavage in the radical mechanism as well as in the nonradical mechanism. Considering such a small activation energy for the H-atom abstraction, the collision of FeO^+ and benzene in a proper orientation can cause the H-atom abstraction via TS3. However, this H-atom abstraction step lies 7.9 kcal/mol above the corresponding one in the nonradical mechanism on the low-lying quartet potential energy surface. Although the first pathway contains a high barrier of more than 30 kcal/mol, we conclude that the nonradical mechanism is more likely to occur in the gas-phase reaction by FeO^+.[17] We think that the energy of the transition state for H-atom abstraction (relative to the dissociation limit) should play a dominant role rather than the corresponding activation barrier. Since the B1 minimum in the first pathway is energetically the deepest one, the corresponding activation barrier for H-atom abstraction is large, but the present reaction does not involve thermodynamical equilibrium. The nonradical mechanism is applicable when the metal center of catalytic active sites is coordinatively unsaturated, as previously discussed in benzene hydroxylation over Fe−ZSM-5 zeolite.[30]

The second half of the radical pathway is responsible for the formation of the phenol complex via TS4, which has an imaginary frequency of 139i cm^{-1} in the sextet state and 499i cm^{-1} in the quartet state. These low-frequency modes mean that the interaction between the carbon radical center and the O atom of the FeOH moiety is weak. The C−O bond distance is calculated to be 2.719 and 2.686 Å in the sextet and quartet states, respectively. The activation energy for the radical rebound step is 12.4 kcal/mol in the sextet state and 3.3 kcal/mol in the quartet state. Therefore the reacting system should proceed on the quartet potential energy surface in the final stages of the reaction.

Oxygen-Insertion Mechanism. Let us next look at the oxygen-insertion mechanism, in which an arenium intermediate (A) is formed via oxygen insertion into the benzene ring. Figure 3 shows computed energy diagrams along the reaction pathway of this mechanism. A benzene complex (B3), which has a nonplanar geometry with a direct interaction between the benzene ring and the oxygen atom of FeO^+, is initially formed in the oxygen-insertion mechanism. After that, complex B3 undergoes a direct attack of the oxygen atom to form intermediate A with a C−O bond via a transition state (TS5). The activation energy for this oxygen-insertion step is only 0.1 kcal/mol on the quartet surface and 0.6 kcal/mol on the sextet surface, indicating that this reaction is substantially barrierless. This is due to the early transition state; in other words, the transition-state structure is very similar to the structure of B3. Thus, complex B3 can easily go to intermediate A, the insertion step being downhill with an exothermal energy of 20.4 kcal/mol on the sextet surface and 9.2 kcal/mol on the quartet surface. It is therefore reasonable that we assume the oxygen-insertion mechanism to start from intermediate A. In view of the C−O distances in B3 and TS5 in both spin states, the benzene ring is loosely bound to the FeO moiety in the sextet state compared to that in the quartet state. The structure of intermediate A can be viewed as a σ complex, a highly reactive intermediate in aromatic electrophilic substitution. The formation of this complex causes a significant deformation of the benzene ring, the resultant quinoid structure having two C=C double bonds of 1.377 Å (not shown in Figure 3). This ring deformation is consistent with the Mulliken population analysis (summarized in Table 2) that calculated atomic charges on the *para*-position carbon atom and the oxygen atom are +0.28 and −0.39 in the quartet state, respectively.

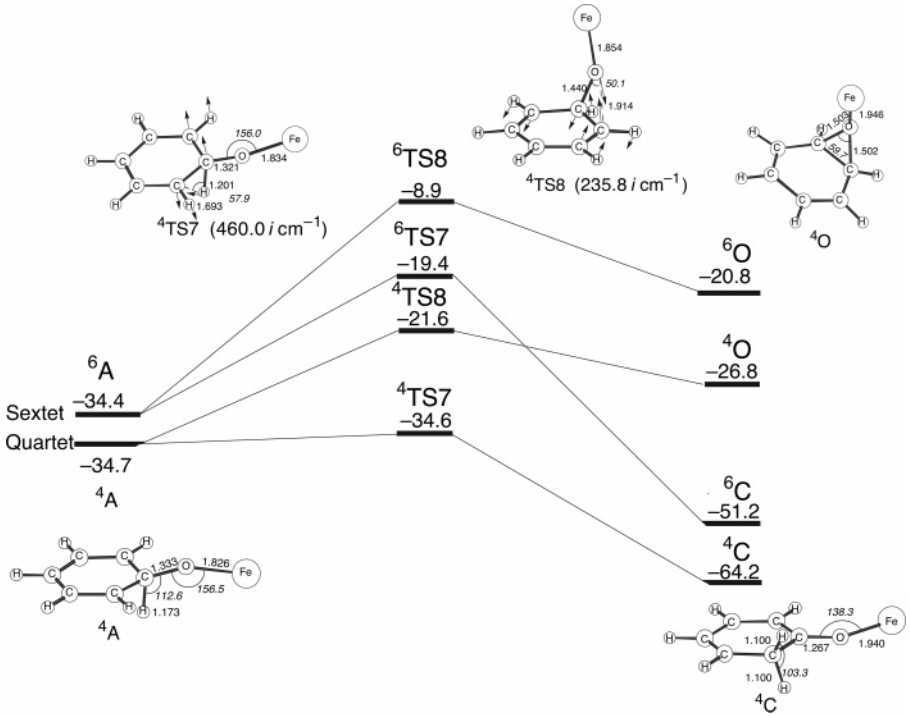

Figure 4. Energy diagrams for the formation of cyclohexadienone and benzene oxide in the oxygen-insertion mechanism at the B3LYP level of theory. Units are in kcal/mol.

Table 2. Calculated Mulliken Atomic Charges for the Reaction Species in the Oxygen-Insertion Mechanism (values in parentheses are atomic spin densities)

entry	B3	TS5	A	TS6	TS7	C	TS8	O
sextet								
Fe	0.69	0.76	0.68	0.59	0.56	0.62	0.59	0.60
	(3.73)	(3.89)	(4.36)	(4.84)	(4.95)	(4.99)	(4.89)	(4.93)
O	−0.07	−0.12	−0.24	−0.31	−0.33	−0.21	−0.11	−0.07
	(0.75)	(0.51)	(0.16)	(−0.02)	(0.00)	(−0.04)	(−0.06)	(−0.05)
substrate	0.38	0.36	0.56	0.72	0.77	0.59	0.52	0.47
	(0.52)	(0.60)	(0.48)	(0.18)	(0.05)	(0.05)	(0.17)	(0.12)
quartet								
Fe	0.81	0.84	0.65	0.70	0.63	0.70	0.65	0.73
	(3.49)	(3.49)	(2.91)	(2.93)	(2.90)	(2.99)	(2.91)	(2.98)
O	−0.24	−0.21	−0.39	−0.43	−0.38	−0.25	−0.33	−0.21
	(0.22)	(0.26)	(0.07)	(0.01)	(0.05)	(−0.03)	(0.00)	(−0.01)
substrate	0.42	0.36	0.73	0.73	0.75	0.55	0.68	0.48
	(−0.72)	(−0.74)	(0.03)	(0.06)	(0.05)	(0.04)	(0.08)	(0.02)

We expect intermediate A to undergo a rearrangement to the phenol complex and found a reaction pathway that directly connects intermediate A and the phenol complex via a transition state (TS6). It is a transition state responsible for the breaking of a C−H bond and the formation of an O−H bond. The quartet potential energy surface for the oxygen-insertion pathway is calculated to lie energetically below the corresponding sextet surface. Calculated activation barriers toward TS6 are 25.2 kcal/mol on the sextet surface and 21.9 kcal/mol on the quartet surface. This reaction step is energetically comparable to the H-atom abstraction step (TS1) in the nonradical mechanism since the oxygen-insertion step via TS5 is barrierless. However, ^{4}TS1 lies well below ^{4}TS6, although ^{6}TS1 is close to ^{6}TS6 in energy. Although the nonradical mechanism is applicable only when the metal active site is coordinatively unsaturated, we can conclude from the energies of the transition states for H-atom abstraction that TS1 is a better route for the effective dissociation of a C−H bond.

Formation of Cyclohexadienone and Benzene Oxide. We found reaction pathways from intermediate A to cyclohexadienone and benzene oxide, as indicated in Scheme 1. Figure 4 shows computed energy diagrams from A to the cyclohexadienone complex (C) and the benzene oxide complex (O). Let us first look at the production of complex C. One of the benzene C−H bonds activated by the oxygen attack is cleaved, and then the H atom is shifted to the neighboring *ortho* carbon atom via a transition state (TS7). These processes result in the formation of complex C. The energy splitting between the quartet and sextet surfaces significantly increases from 0.3 kcal/mol in A to 15.2 kcal/mol in TS7. As a result, calculated activation energies for the H atom shift are 15.0 kcal/mol in the sextet state and 0.1 kcal/mol in the quartet state. Considering that the H atom shift via ^{4}TS6 requires 21.9 kcal/mol as an activation energy to form the phenol complex, the formation of complex C can easily take place via intermediate A with no cost of energy. This is an important reaction pathway for benzene hydroxylation.

Finally we would like to address the ring-closure step responsible for the formation of benzene oxide via TS8, which is a transition state for the formation of an epoxide ring. This reaction pathway is relatively unimportant from the energetic point of view. Calculated activation energies for the ring closure are 25.5 kcal/mol on the sextet surface and 13.1 kcal/mol on the quartet surface. Moreover, the reaction energy for the ring-closure step in the sextet and quartet states is 13.6 and 7.9 kcal/mol endothermic, respectively. Therefore the formation of complex O is unlikely to occur in the reaction between benzene and FeO^+. Although this reaction pathway has been repeatedly invoked to explain the mechanism of benzene hydroxylation, it can be ruled out because benzene oxide is energetically unstable owing to the destruction of the resonant structure of the benzene ring.

Schwarz and co-workers[9] suggested that although phenol and cyclohexadienone are tautomers, the keto−enol transformation is forbidden on the experimental time scale of the gas-phase reaction between FeO^+ and benzene. They considered that various products such as $Fe^+ + C_6H_5OH$, $Fe^+(C_6H_4) + H_2O$, and $Fe^+(C_5H_6) + CO$ in the reaction should come from $HO-Fe^+-C_6H_5$, cyclohexadienone, and/or benzene oxide. The present computational result that the nonradical pathway is a major branch compared to the oxygen-insertion pathway via cyclohexadienone is consistent with the experimental findings. In contrast, Shaik and co-workers[18] proposed that benzene hydroxylation by cytochrome P450 should occur via the formation of cyclohexadienone. Since the active species of P450 (compound I) is a six-coordinate iron-oxo porphyrin π cation radical, the reaction pathway via cyclohexadienone is quite reasonable. Enzymatic phenylalanine hydroxylation is also explained on the basis of the mechanism via cyclohexadienone.[32,33]

Panov and co-workers[14] demonstrated that in the hydroxylation of 1,3,5-d_3-benzene over Fe−ZSM-5 zeolite the deuterium-labeled sites are completely retained in product phenols. No deuterium shift was observed in this reaction, which suggests that the zeolite-catalyzed reaction does not involve cyclohexadienone as an intermediate. Since the formation of benzene oxide is energetically unfavorable, the oxygen-insertion mechanism is not appropriate in benzene hydroxylation over Fe−ZSM-5 zeolite. Therefore we propose that this catalytic reaction should take place in a nonradical manner as in the gas-phase reaction if the α-oxygen species is coordinatively unsaturated as we proposed previously.[30]

(32) Bassan, A.; Blomberg, M. R. A.; Siegbahn, P. E. M. *Chem. Eur. J.* **2003**, *9*, 106.
(33) Shiota, Y.; Yoshizawa, K. *J. Phys. Chem. B* **2004**, *108*, 17226.

Conclusions

We have discussed possible mechanisms for the direct oxidation of benzene to phenol catalyzed by the bare FeO^+ complex in the gas phase. Three reaction pathways are available: one is a nonradical mechanism to form a hydoroxo intermediate, $HO-Fe^+-C_6H_5$, the second is a radical mechanism that forms a phenyl radical and an FeOH fragment as an intermediate, and the third is an oxygen-insertion mechanism that forms an arenium intermediate. The H-atom abstraction step is the rate-determining step in each mechanism. The energies of the transition states with respect to H-atom abstraction increase in the order of the first, third, and second mechanisms. This analysis of the potential energy surfaces shows that the first mechanism is the most favorable in energy when the metal active site is coordinatively unsaturated. The second mechanism is energetically unlikely in the reaction by FeO^+. The third pathway is branched into cyclohexadienone and benzene oxide, which are formed by a 1,2-hydrogen migration and a ring closure in the arenium intermediate, respectively. The formation of cyclohexadienone from the arenium intermediate is another possible pathway for benzene hydroxylation when the metal active site is coordinatively saturated. In acidic and neutral solutions the conversion of cyclohexadienone to phenol can easily occur through the keto−enol tautomerization. Thus, the cyclohexadienone complex also plays a role in the formation of the final phenol product as a transient intermediate. In contrast, the formation of benzene oxide is not allowed under ambient conditions because of its extremely high energy, due to the destruction of the resonant structure of the benzene ring. The DFT calculations lead us to conclude that the nonradical mechanism is a major branch among the three mechanisms. However, the present reaction does not involve thermodynamical equilibrium. Classical trajectory calculations are probably useful for a more detailed discussion.

Acknowledgment. K.Y. acknowledges the Ministry of Culture, Sports, Science and Technology of Japan, Japan Society for the Promotion of Science, and CREST of Japan Science and Technology Cooperation for their support of this work.

Supporting Information Available: Figures S1, S2, S3, and S4 of optimized geometries along the reaction pathways for the direct oxidation of benzene. This material is available free of charge via the Internet at http://pubs.acs.org.

OM050136B